GeoHealth

RESEARCH ARTICLE

10.1029/2024GH001039

Satellite-Derived, Smartphone-Delivered Geospatial Cholera Risk Information for Vulnerable Populations

Farah Nusrat[1,2], Ali S. Akanda[2], Abdullah Islam[3,4], Sonia Aziz[5], Emily L. Pakhtigian[6], Kevin Boyle[7], and Syed Manzoor Ahmed Hanifi[8]

[1]Southwest Climate Adaptation Science Center, Utah State University, Logan, UT, USA, [2]Department of Civil and Environmental Engineering, University of Rhode Island, Kingston, RI, USA, [3]Department of Computer Science and Statistics, University of Rhode Island, Kingston, RI, USA, [4]Foursquare, Inc., Seattle, WA, USA, [5]School of Business and Economics, Moravian University, Bethlehem, PA, USA, [6]School of Public Policy, Pennsylvania State University, State College, PA, USA, [7]Pamplin College of Business, Virginia Polytechnic Institute and State University, Blacksburg, VA, USA, [8]International Centre for Diarrhoeal Disease Research, Dhaka, Bangladesh

Abstract Cholera, an acute waterborne diarrheal disease, remains a major global health challenge. Despite being curable and preventable, it can be fatal if left untreated, especially for children. Bangladesh, a cholera-endemic country with a high disease burden, experiences two peaks annually, during the dry pre-monsoon spring and the wet post-monsoon fall seasons. An early warning system for disseminating cholera risk, which has potential to reduce the disease burden, currently does not exist in Bangladesh. Such systems can raise timely awareness and allow households in rural, riverine areas like Matlab to make behavioral adjustments with water usage and around water resources to reduce contracting and transmitting cholera. Current dissemination approaches typically target local government and public health organizations; however, the vulnerable rural populations largely remain outside the information chain. Here, we develop and evaluate the accuracy of an early warning system—CholeraMap that uses high-resolution earth observations to forecast cholera risk and disseminate geocoded risk maps directly to Matlab's population via a mobile smartphone application. Instead of relying on difficult to obtain station-based environmental and hydroclimatological data, this study offers a new opportunity to use remote sensing data sets for designing and operating a disease early warning system. CholeraMap delivers monthly, color-coded geospatial maps (1 km × 1 km spatial resolution) with household and community cholera risk information. Our results demonstrate that the satellite-derived local-scale risk model satisfactorily captured the seasonal cholera pattern for the Matlab region, and a detailed high-resolution picture of the spatial progression of at-risk areas during outbreak months.

Plain Language Summary Cholera, an acute waterborne diarrheal disease, remains a major public health challenge in developing nations. An early warning system for disseminating cholera risk has the potential to reduce the disease burden in rural, riverine, and endemic countries like Bangladesh. Current dissemination approaches typically target local government and public health organizations but largely overlook the vulnerable rural populations. We develop and evaluate the accuracy of an early warning system—CholeraMap that uses satellite remote sensing data to forecast cholera risk and disseminate geocoded risk maps directly to the remote population of Matlab, Bangladesh via a mobile smartphone application. CholeraMap delivers monthly, color-coded risk maps to provide users with household and community cholera risk information along with associated explanations of the risks. Our results satisfactorily captured the spatiotemporal progression of at-risk areas during high outbreak months and were disseminated to the vulnerable population of Matlab via this novel smartphone application.

Key Points:

- An early warning system for disseminating cholera risk has the potential to reduce disease burden in vulnerable endemic populations
- This study is the first attempt to combine satellite data sets and smartphone-based dissemination for waterborne diarrheal disease applications
- CholeraMap captured the spatiotemporal patterns and high-resolution view of the progression of cholera risk during outbreak months

Supporting Information:

Supporting Information may be found in the online version of this article.

Correspondence to:

A. S. Akanda,
akanda@uri.edu

Citation:

Nusrat, F., Akanda, A. S., Islam, A., Aziz, S., Pakhtigian, E. L., Boyle, K., & Hanifi, S. M. A. (2024). Satellite-derived, smartphone-delivered geospatial cholera risk information for vulnerable populations. *GeoHealth*, *8*, e2024GH001039. https://doi.org/10.1029/2024GH001039

Received 21 FEB 2024
Accepted 28 SEP 2024

Author Contributions:

Conceptualization: Ali S. Akanda, Sonia Aziz, Emily L. Pakhtigian, Kevin Boyle
Data curation: Farah Nusrat, Ali S. Akanda, Abdullah Islam, Emily L. Pakhtigian, Syed Manzoor Ahmed Hanifi
Formal analysis: Farah Nusrat, Ali S. Akanda, Abdullah Islam, Sonia Aziz, Emily L. Pakhtigian, Kevin Boyle
Funding acquisition: Sonia Aziz

1. Introduction

Cholera is an acute waterborne diarrheal disease, contracted by ingesting the bacterium *Vibrio cholerae* that causes rapid dehydration and electrolyte imbalance (Baker-Austin et al., 2018; Farmer et al., 2011; Hiremath et al., 2015; Sack et al., 2004). There is a 50% case-fatality rate if people are left untreated for more than 24 hr (Farmer et al., 2011; Sack et al., 2004). The major transmission path is the fecal-oral route—where consumption of food or water is contaminated with the feces of an infected person (Abdulrahim & Adesola, 2022; Sit et al., 2022). The World Health Organization (WHO) defines a cholera-endemic country as one with a history of local cholera transmission in the last 3 years rather than importing cholera from other locations (Craig, 2018;

Investigation: Ali S. Akanda, Sonia Aziz, Emily L. Pakhtigian, Syed Manzoor Ahmed Hanifi
Methodology: Farah Nusrat, Ali S. Akanda, Sonia Aziz, Emily L. Pakhtigian
Project administration: Ali S. Akanda, Sonia Aziz
Resources: Ali S. Akanda, Abdullah Islam
Software: Farah Nusrat, Ali S. Akanda, Abdullah Islam, Sonia Aziz, Emily L. Pakhtigian
Supervision: Ali S. Akanda, Kevin Boyle, Syed Manzoor Ahmed Hanifi
Validation: Farah Nusrat, Ali S. Akanda, Abdullah Islam
Visualization: Ali S. Akanda
Writing – original draft: Farah Nusrat, Ali S. Akanda
Writing – review & editing: Farah Nusrat, Ali S. Akanda, Abdullah Islam, Sonia Aziz, Emily L. Pakhtigian, Kevin Boyle, Syed Manzoor Ahmed Hanifi

Gabutti et al., 2020; WHO, 2022). In the 69 countries in which cholera is endemic, approximately 1.3 billion people are at risk of the disease, and there are approximately 2.86 million annual cases (Ali et al., 2015). In the cholera-endemic Ganges Delta region, Bangladesh is one of the countries with the highest number of people at risk for cholera, resulting in over 100,000 cases and 1,000 fatalities annually (Ali et al., 2015; Sack et al., 2021).

Recent studies found both water abundance (flooding) and shortage (drought) contribute to cholera outbreaks (Levy et al., 2016). In water supply and sanitation-deprived regions in Africa, both high and low rainfall events in dry areas are associated with higher cholera incidence; however, in wetter areas, high rainfall is associated with lower cholera incidence (Moore et al., 2017). Rainfall impacts cholera transmission in two ways: (a) low rainfall increases pathogen concentration in waterbodies; and (b) high rainfall worsens sanitation conditions due to high rainfall generated runoff, which increases the pathogen load in water bodies (e.g., spillover of pit latrines, washouts of open defecation places) (Gaudart et al., 2013; Lloyd et al., 2007; Moors et al., 2013; Ruiz-Moreno et al., 2007; Singh et al., 2001). In areas with compromised water, sanitation, and hygiene (WASH) infrastructure, high-intensity rainfall increases the risk of cholera transmission contaminating drinking water systems with sewage, leading to higher cholera cases that begin about a month after the start of the rainy season (Rinaldo et al., 2012; Taneja et al., 2020). In Zanzibar, which has a tropical monsoon climate, an increase of 200 mm of rainfall was associated with a 1.6-fold rise in cholera cases, following a 2-month lag (Reyburn et al., 2011). However, another WASH-deprived country, Yemen, which has an arid subtropic climate, experienced a positive association between weekly rainfall and a shorter lag period for cholera—about 10 days (Camacho et al., 2018). Low rainfall increases the concentration of harmful pathogens and wastewater elements in water sources, which reduces the water quality and increases the risk of human contact with pathogens (Levy et al., 2016; Moors et al., 2013; Moran et al., 1997; Shehane et al., 2005). Although, a study for the Matlab region in Bangladesh found no influence of rainfall on cholera occurrence between 1988 and 2001 (Ali et al., 2013). In Bangladesh, rainfall and cholera cases are found to be negatively correlated during spring, given high cholera transmission during the dry spring season (Akanda et al., 2009; Koelle et al., 2005).

Temperature ranges between 28 and 34°C (31 ± 3°C) facilitate the development and reproduction of pathogens, leading to higher cholera occurrence (Alam et al., 2007; Asadgol et al., 2019; Batabyal et al., 2014; Saha et al., 2019; Silva & Benitez, 2016). Moreover, an increase in temperature causes higher evaporation, resulting in lower water levels in water bodies. As pathogen concentration increases with water scarcity, cholera outbreaks may increase as well (Jutla et al., 2013). Approximately 50% of all cholera outbreaks occur when the temperature is greater than 31°C (Asadgol et al., 2020; Jutla et al., 2013). For example, a study in north India found a 1-month lag between having a high temperature (greater than 30°C during the summer months) and higher cholera cases (Taneja et al., 2020). Another study for epidemic regions found a higher likelihood of cholera outbreaks when air temperature stays higher than the climatological average for 2 months or more, followed by heavy rainfall (Jutla et al., 2013). A time series analysis for Matlab, Bangladesh (1988–2001) found a 6% increase in cholera cases concurrent with a 1°C increase in minimum temperature (Ali et al., 2013). Other studies of the Matlab region also find higher cholera cases during periods of increased temperatures (Ali et al., 2013; Emch et al., 2008; Islam et al., 2009). During such times, the water temperature of shallow waterbodies can easily increase with the rising Land Surface Temperature (LST), generating a suitable environment for the growth of *V. cholerae* (Khan et al., 2019; Pascual et al., 2000). LST was found to be an important contributor to cholera outbreaks in New Delhi, India (Elnemr, 2014). A study for coastal India found that monthly LST in the month of a cholera outbreak plays an important role as a predictor of that outbreak (Campbell et al., 2020; Jutla et al., 2013).

Elevation is an additional factor in determining cholera risk as low-elevation areas are more flood-prone, which increases the chances of contact between people and water contaminated with the vibrio (Smirnova et al., 2020; Xu et al., 2016). Lower elevation areas near rivers are usually flooded by high discharge flow volumes during the rainy season. After heavy rainfall or floods, low-lying lands that lack proper drainage or sewer systems experience water stagnation, hampering the sanitation system, and accelerating cholera outbreaks (Luque Fernandez et al., 2012; Zarocostas, 2009). In Zimbabwe, a 30% decrease in cholera risk was observed with every 100 m increase in elevation (Luque Fernandez et al., 2012). In lower elevations, people without adequate water supply and sewage disposal systems rely on unprotected shallow wells, which can easily be contaminated with sewage, putting more people at disease risk (Luque Fernandez et al., 2012; Mason, 2009). In addition, sea level rise can cause saline water intrusion in low-lying areas, which increases the likelihood of waterborne pathogen transmission (Christaki et al., 2020; Costello et al., 2009; Dvorak et al., 2018). The increasing salinity also allows a

more hospitable environment for the growth of *V. cholerae* (Huq et al., 1984, 2005; Jutla et al., 2013; Louis et al., 2003; Tamplin et al., 1990).

Population density is an important risk factor in the transmission of cholera (Griffith et al., 2006; Siddique et al., 1992). High population density puts extra pressure on existing water, sanitation, and health, generating a suitable environment for waterborne diarrheal disease outbreaks and transmission (Ali et al., 2002; Finger et al., 2016; Root, 1997; Siddique et al., 1992). Positive correlations among population density, poor sanitation facilities, and cholera incidence rates have been observed across many developing regions (Ali et al., 2002). People living in densely populated developing or underdeveloped regions typically lack clean water supply and sanitation systems and often rely on unimproved sanitation options such as shared facilities and open defecation (Finger et al., 2016).

In an endemic setting, cholera outbreaks are observed in a recurrent manner in both space and time (Codeço, 2001). The risk of cholera cannot be fully eradicated as the causative agent (*V. cholerae*) is native to aquatic settings in many tropical regions (Jutla et al., 2013, 2015). It can survive in aquatic environments in a viable but non-culturable (VBNC) form, which can cause an outbreak after finding a suitable environment (Chamanrokh et al., 2022; Codeço, 2001; Colwell et al., 1996). In Bangladesh, cholera occurs around the year but exhibits distinct seasonal outbreaks, a smaller outbreak in the spring (March–May) season and a larger one in the post-monsoon (October–November) season (Akanda et al., 2009, 2013; Alam et al., 2011; Hashizume et al., 2010; Lobitz et al., 2000). The spring cholera peak is associated with low rainfall and water scarcity whereas, the post-monsoon cholera peak is associated with high rainfall and flood inundation (Hashizume et al., 2010). Dry season flows in the Ganges and Brahmaputra Rivers are inversely associated with increased cholera cases during the spring season, while monsoon-induced flows and flood inundation lead to increased cholera during the post-monsoon season (Akanda et al., 2009).

Early warning systems can help reduce the disease burden even if it cannot be completely eradicated. Such a system provides notification of a possible disease outbreak in a location to the local population and public health officials well in advance of the threat to allow time for preventative behaviors and proactive response options (Council, 2001). Such an early warning system may also have the capacity to regularly monitor catalysts impacting disease outbreaks and predictively model the risk of outbreaks (Hussain-Alkhateeb et al., 2021; Nusrat, Haque, et al., 2022; Nusrat, Khan, et al., 2022). Instead of using one model for a large geographic location (e.g., country), the model's scale needs to be local or regional to incorporate native features in those models for better representation (Constantin de Magny et al., 2008). Location-specific early warning systems are typically robust as they incorporate the influence of local environmental and social features on disease outbreaks for better prevention and management (Chou et al., 2010). Moreover, these early warning systems can aid in the targeted dispersion of public health resources and the design of public health policies (Chou et al., 2010; Constantin de Magny et al., 2008).

In this study, we developed and deployed a cholera early warning system for the Matlab subdistrict region in Bangladesh, which did not employ any such system previously. We employed a geospatial cholera risk model that uses satellite-derived observations including rainfall, temperature, population density, and elevation. We used the outputs of this model to populate a smartphone application that communicates these risk predictions and other cholera-related information directly to the stakeholder population. This study is a novel attempt to combine the powers of satellite remote sensing data sets and dissemination via smartphones for waterborne diarrheal diseases or water-related health applications. The primary objectives of this study are to: (a) develop a modeling framework for a high-resolution (1 km × 1 km) cholera early warning system using geospatial data and remote sensing earth observations for the area of Matlab; and (b) disseminate geographically personalized and temporally dynamic cholera risk predictions including preventive measures directly to local populations in a simple and user-friendly smartphone application.

2. Methodology

2.1. Study Area

This study focuses on Matlab, a cholera-endemic rural upazila (sub-district) in the Chandpur district of Bangladesh that is situated 250 km upstream from coastal regions and 50 km south-east of Dhaka, the capital (Alam et al., 2011, 2017). The population in a 484 square kilometer (km) region (22 km × 22 km) of this upazila

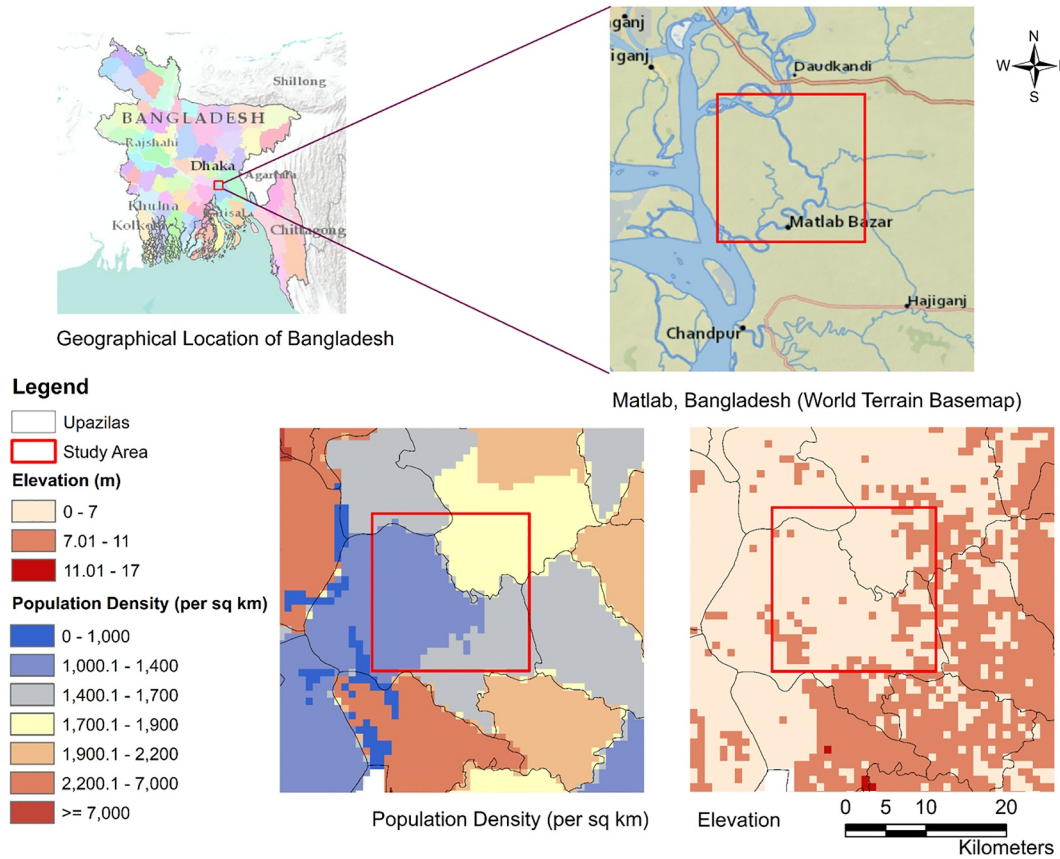

Figure 1. Study area (Matlab, Bangladesh).

was chosen for the dissemination of the early warning system through the smartphone application (Figure 1). The study area is situated north of the confluence of the Padma (combined flow of the Ganges and the Brahmaputra) and Meghna rivers (Carrel et al., 2010). The region is mostly flat, with an elevation below 7 m above sea level across most of the study region, and between 7 and 11 m in eastern parts of Matlab. During the monsoon months, this location floods regularly (Akanda et al., 2013; Alam et al., 2017).

The issue of floods is critical for Bangladesh due to its devastating impacts on waterborne diseases (Palash et al., 2018). The post-monsoon cholera peak is directly influenced by floods in many areas of Bangladesh (Akanda et al., 2009, 2011). However, the population living in Matlab is largely protected by flood control embankments constructed in 1988 (Carrel et al., 2010). In addition, due to its advantageous location north of the confluence of the big rivers, the floods in the Matlab area are typically of smaller nature, and more induced by local heavy rainfall than river flooding from upstream flows (Manandhar et al., 2020).

There are three dominant seasons—winter (November–February), spring (March–May), and monsoon (June–September) (Alam et al., 2017; Anjumand, 2011). Monthly rainfall varies from 0 to 540 mm with a monthly average of 138 mm, and air temperature varies between 20 and 34°C with a monthly average of 27°C (Call et al., 2017). Dual cholera peaks are observed in Matlab; a smaller peak occurs during spring (March–May) and a larger peak occurs during post-monsoon months (September–December) (Akanda et al., 2013; Ali et al., 2013; Emch et al., 2010; Longini Jr et al., 2002). Figure 2 shows the monthly climatology of rainfall and Land Surface Temperature (LST) patterns in Matlab based on 20 years of observations (2000–2020).

The International Center for Diarrheal Disease Research, Bangladesh (icddr,b) operates two health facilities in Matlab—Health and Demographic Surveillance System (HDSS) and Matlab Hospital (Brooks et al., 2021). There are 7 administrative blocks for Matlab (icddr,b service blocks—A, B, C, D, and government services blocks—E, F, G) (Haq et al., 2018; Pakhtigian et al., 2022). Our study area falls within the northern part of Matlab upazila, which consists of government service blocks E, F, and G (Pakhtigian et al., 2022). As of 2022, Matlab has a total

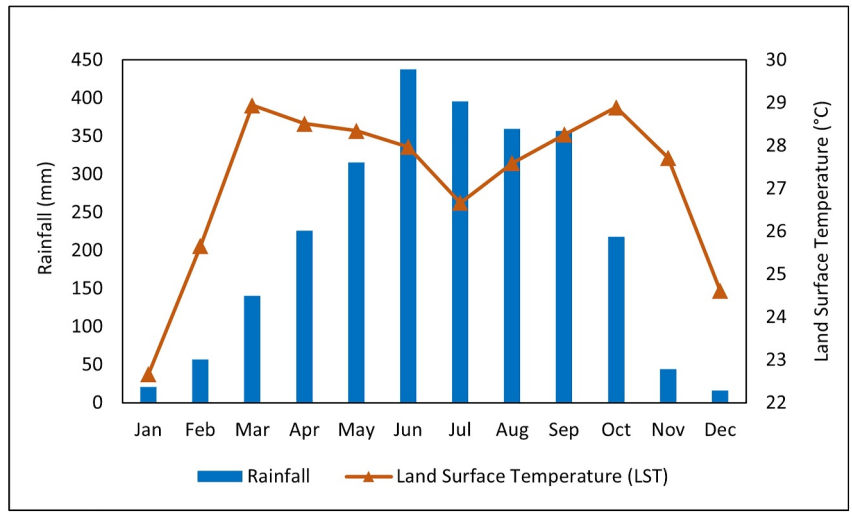

Figure 2. Climatology of Rainfall (IMERG) and Land Surface Temperature (MODIS) of Matlab (2000–2020).

population of approximately 247,000 people and the population density ranges between 1,200 and 1,800 persons per km^2.

2.2. Data Sources

Remote sensing data sets from multiple satellite missions and gridded land surface and demographic data sets from global depositories are used in this study. To predict cholera risk index for any month, we bring together data on population density, elevation, previous month's rainfall, and LST anomaly, previous month's average cholera prevalence (2016–2019), and forecasted rainfall and temperature of that month. Population density and elevation data were collected from Socioeconomic Data and Applications Center (SEDAC) and USGS respectively. Monthly rainfall and LST anomalies (difference between monthly value and the average of the long-term value for the same period) were calculated using the Integrated Multi-satellitE Retrievals for GPM (IMERG) and Moderate Resolution Imaging Spectroradiometer (MODIS) data respectively. Rainfall and temperature forecasted data were collected from NOAA's North American Multi-Model Ensemble (NMME) project's Community Climate System Model (CCSM). NMME is a forecasting system with 10 ensembles that provides real-time seasonal forecasts up to 180 days in advance (Kirtman et al., 2014). These multi-model ensembles were used in this study as they deliver more advanced quality forecasting than any single-model ensemble (Doblas-Reyes et al., 2005; Hagedorn et al., 2005; Kirtman & Min, 2009; Slater et al., 2017). We used recent cholera prevalence data (ratio of cholera patients and total diarrheal patients in a hospital) from 2016 to 2019 for model building, and we used publicly available data sets from 1998 to 2007 for validation (Akanda et al., 2011; IEDCR, 2022) to see how the timing and magnitude of recent cholera peaks match historical cholera patterns. The details of data sources and types, spatial resolutions, and the weightage of each variable used in this model are given in Table 1.

2.3. Geospatial Risk Model

We developed a weighted sum geospatial model to determine the cholera risk index using environmental and socioeconomic variables. A weighted sum model is typically used for evaluating a number of alternative scenarios with assigned weights for each. In this geospatial version, the model was set over a 22 km × 22 km region with each cell (1 km × 1 km) representing the combined risk values of that location based on the environmental variables and their assigned weights. We first examined the impact of each environmental variable on monthly cholera risk using a lag correlation analysis (Table S1 in Supporting Information S1). The static variables (elevation and population density) were not included in this analysis. The risk model was then prepared using the predictors, with each variable assigned a specific weightage (Table 1).

We put equal weightage at the start of the selected set of hydroclimatic, land surface, and socioeconomic variables. We then used a trial-and-error approach to capture the influence of each variable and correlate with past cholera data to ensure that our model can capture the seasonal cholera risk patterns. We further diversified the

Table 1
Data Types, Sources, Spatial Resolutions, and Variable Weightage in the Model

Types	Variables	Sources	Spatial resolution	Variable weightage (%)
Social	Population Density (2020)	Socioeconomic Data and Applications Center (SEDAC)[a]	1 km × 1 km	20
Topographic	Elevation	USGS HydroSHEDS[b]	1 km × 1 km	10
Environmental (Preceding)	Monthly rainfall anomaly	Integrated Multi-satellitE Retrievals for GPM (IMERG)[c]	~10 km × 10 km	15
	Monthly LST anomaly	Moderate Resolution Imaging Spectroradiometer (MODIS)[d,e]	~1 km × 1 km	10
Epidemiological (Preceding)	Monthly Average Cholera Prevalence	Institute of Epidemiology, Disease Control and Research (IEDCR), Dhaka, Bangladesh[f]	Surveillance data from 22 Hospitals were converted to 1 km × 1 km layers	20
Environmental (Forecasting)	Monthly total Rainfall of upcoming month	North American Multi-Model Ensemble (NMME) Community Climate System Model (CCSM4)[g]	~50 km × 50 km	15
	Monthly average Temperature of upcoming month			10

[a]CIESIN (Center for International Earth Science Information Network)—Columbia University (2018). "Gridded Population of the World, Version 4 (GPWv4): Population Density, Revision 11." [b]Lehner et al. (2008). "New Global Hydrography Derived from Spaceborne Elevation Data." [c]Huffman et al. (2019) "GPM IMERG Late Precipitation L3 1 Day 0.1 Degree × 0.1 Degree V06, Edited by Andrey Savtchenko." [d]Wan et al. (2015). "MOD11C3 MODIS/Terra Land Surface Temperature/Emissivity Monthly L3 Global 0.05Deg CMG V006 [Data Set]." [e]Wan et al. (2021). "MODIS/Terra Land Surface Temperature/Emissivity Daily L3 Global 1 km SIN Grid V061 [Data Set]." [f]IEDCR (Institute of Epidemiology, Disease Control and Research, Dhaka, Bangladesh) (2022). Ongoing Surveillance. (https://old.iedcr.gov.bd/index.php/surveillance). [g]Kirtman et al. (2014). "The North American Multi-Model Ensemble (NMME): Phase-1 seasonal to interannual prediction; Phase-2 toward developing intra-seasonal prediction."

weightage based on literature evidence and our understanding of the model's performance improvement and matched it with past cholera data (Akanda et al., 2009, 2011, 2013; Nusrat, Haque, et al., 2022; Nusrat, Khan, et al., 2022).

First, each variable was classified as different risk layers (risk 0 to risk 4) according to its values. Then the risk values for each variable were summed into one single raster risk layer and included in the weighted sum model. The final output of the weighted sum model was then rescaled between 0 and 1 by normalizing all risk values (0–4) with respect to the highest risk value (4). The rescaled risk values were divided into three groups: low (0.00–0.30), medium (0.31–0.60), and high (0.61–1.00). Low, medium, and high risks were represented with green, yellow, and red colors, respectively, in the risk maps generated for the early warning system for easier interpretation of cholera risk intensity. Figure 3 shows the conceptual structure and the flowchart of the monthly cholera risk model.

Our study aims to utilize the most readily available satellite earth observations data sets to create a cholera risk forecasting model that can help local people in decision-making. However, while selecting the spatial scale of the model, we need to strike a balance between the advantages of the community scale and the much larger synoptic scales of hydroclimatic variables and processes. Past modeling efforts in this region have focused on hydroclimatic influences on cholera outbreaks at 0.1–0.5° scales, roughly 10–50 km (Akanda et al., 2011; Jutla et al., 2013; Khan et al., 2017). Recent studies focusing on Yemen and Malawi have provided cholera risk at 1 km × 1 km resolution (Jutla et al., 2023; Usmani et al., 2023). Our effort is built for a rural area where major water sources (ponds, rivers, canals, tubewells, etc.) could be similar within near distances (<1 km) and the hydroclimatic drivers do not show much variability at those scales. In addition, the target communities live in households that are clustered in villages typically situated a few kilometers apart from each other. Therefore, we selected a 1 km × 1 km scale for this model.

Rainfall, which is a major contributor to cholera outbreaks, was used as a proxy for water availability and was assigned the highest importance as a risk factor in the model (Ali et al., 2013). Temperature was another important variable for cholera in Matlab. Rainfall and LST anomalies (the difference between monthly value and the average of the long-term value for the same period) are used in this study, where positive anomaly means wetter (rainfall) or warmer (temperature) months than climatology and vice versa (Hussain-Alkhateeb et al., 2021;

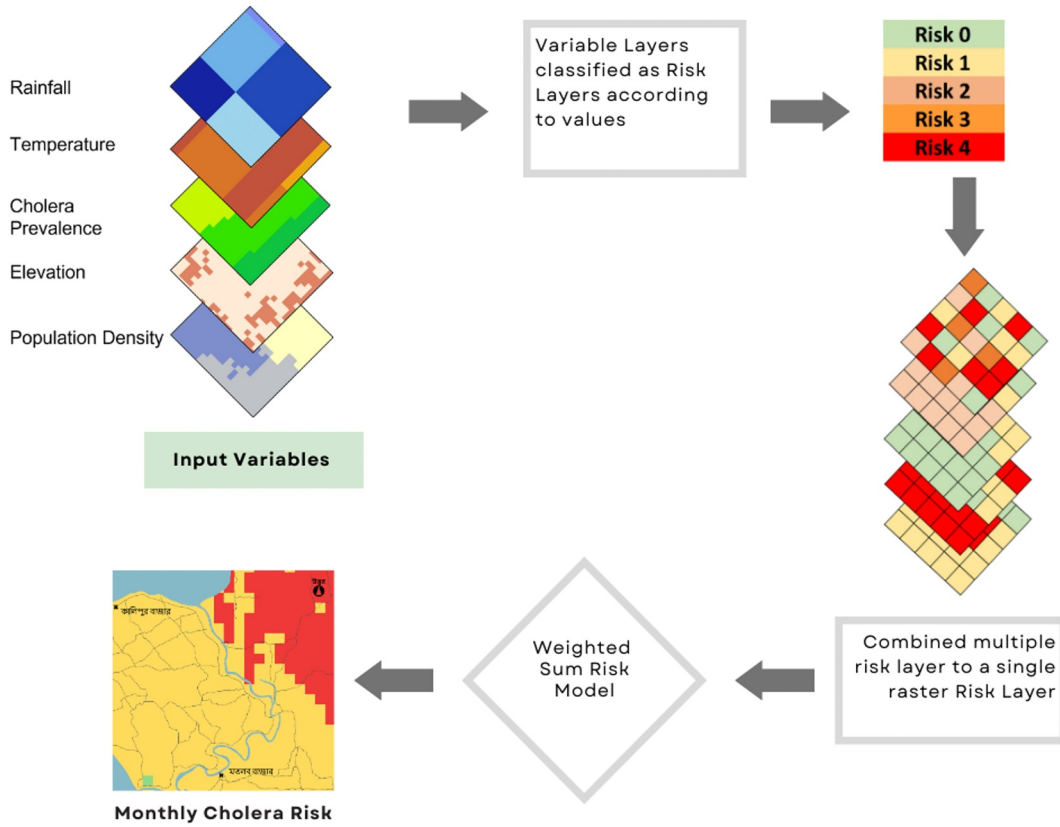

Figure 3. Flowchart of the monthly cholera risk model.

Nusrat, Haque, et al., 2022; Nusrat, Khan, et al., 2022). A 1-month lag is used as it typically takes approximately 1 month for an outbreak to erupt after humans are exposed to the pathogen (Khan et al., 2017). For forecasting cholera using a multi-variable model, environmental variables with a 1-month lag produced the best results and had the lowest Akaike Information Criterion (AIC) and Bayesian Information Criterion (BIC) error rates (Daisy et al., 2020).

More detailed explanation of the role of each variable such as elevation, and population density are provided in Section 1. Our strategy for cholera risk prediction was not only using the lag effect of variables but also addressing the plausible impact of the upcoming month. For this reason, we used both lagged and forecasted rainfall and temperatures to incorporate the influence of the future rainfall and temperatures on cholera risk for the upcoming month. From hydrological changes to cholera cases in humans, no one data layer alone can explain the complex process, as each data layer has its own contribution to determining cholera risk. Therefore, all environmental variable layers along with population density, elevation, and past cholera prevalence are used in the weighted sum model to identify the combined effect of all data layers together to determine the next month's cholera risk.

As direct measurement of water availability is difficult, rainfall was used as a proxy for water availability (Ali et al., 2013). As both water abundance and shortage have been established as important drivers related to cholera outbreaks (Levy et al., 2016), the highest weightage (30%) was assigned to rainfall among the environmental variables (15% for the concurrent month and 15% for the previous month). Studies show both lagged and concurrent positive correlation between temperature and cholera outbreaks as temperature has a strong influence on the growth and replication of pathogens in water (Alam et al., 2007; Asadgol et al., 2019; Batabyal et al., 2014; Saha et al., 2019; Silva & Benitez, 2016). A lower weightage value (20%: 10% for concurrent month and 10% for previous month) was assigned to temperature compared to rainfall.

The past month's cholera prevalence is also known to have an influence on the current month's cholera risk as the baseline WASH conditions do not typically change within a month, unless due to natural disasters. It was assigned 20% weightage in the model as the past cholera prevalence itself has the capacity to pose a significant risk in

creating a suitable environment for cholera outbreaks. Elevation was assigned a 10% weightage as it is a static layer and more of an indirect measure of flood influence on cholera outbreaks. Finally, a 20% weightage was assigned to population density as higher density can increase vulnerability for waterborne diarrheal disease outbreaks and transmission by adding extra pressure on existing WASH systems (Ali et al., 2002; Finger et al., 2016; Root, 1997; Siddique et al., 1992). Results obtained with the above weightage factors were adjusted using a trial-and-error method based on past climatological cholera evidence for the Matlab region.

2.4. Smartphone Application

As part of this study, we developed a smartphone application named "CholeraMap" to deliver the outputs of the geospatial cholera risk model to the project stakeholders—households in Matlab region, Bangladesh. The Android operating system was chosen for the application (https://developer.android.com/studio) as iOS or iPhone penetration is significantly low in Bangladesh. Most smartphones in rural Bangladesh are built on the Android system, are of Chinese origin hardware with limited specifications, and cost less than $100 US. We procured several local handsets to facilitate app testing and quality checks.

The application was built with three main objectives in mind. They were (a) to directly provide high-level technical content to non-technical users in a simple and user-friendly manner; (b) to communicate and explain the geospatial nature of cholera outbreaks to the app users with respect to their locations and the varying risk levels each month; and (c) to provide important preventative water usage information and safety precautions to strengthen the awareness of the app users against cholera transmission.

The technical content of the application is comprised of a color-coded geospatial cholera risk map for the focus region, the central character of the app (a South Asian village girl), the location of the user's household and necessary map legends with explanations of the color codes. The risk map covered a 484 km^2 region, consisting of geocoded 1 km × 1 km pixels that show the monthly cholera risk category. The map also highlights the location of the user's household with a house icon—placed using the coordinates of the phone's last known location—that draws attention to the cholera risk level in the household's immediate and surrounding locations (Figure 4). The dynamic color-coded map is updated each month with the forecasted cholera risks for that month.

3. Results and Discussion

3.1. Geospatial Cholera Risk Maps

The geospatial cholera risk map outputs for 2021 and 2022 are shown in Figures 5 and 6, respectively. The colors green, yellow, and red refer to low, medium, and high cholera risk respectively, each guided by a range of risk calculated by the model. Thus, the colors shown in a map represent the spatial variation of cholera risk across the 484 cells (each representing an area of 1 km × 1 km). The organization of the colored geocoded pixels can also be used to understand the spatial extent of risk and location of the users in the context of high-risk areas.

A strong pattern observed in our monthly risk maps is the biannual or dual peak nature of cholera outbreaks seen in the Bengal Delta region (Akanda et al., 2009; Sack et al., 2003). The Matlab region is situated close to the confluence and along the floodplain corridor of the Ganges-Brahmaputra-Meghna (GBM) river systems, areas that are particularly known to exhibit the dual peak seasonal cholera pattern of the Bengal Delta (Akanda et al., 2013). The peak months of these outbreaks are clearly visible in the high number of red pixels (high-risk areas) seen in May and October in both years. The gradual rise and fall of the high-risk areas as well as the spatial progression is visible in the spring (March-April-May) and post-monsoon or Fall (October–November) months.

In this study, we analyzed the results and the outputs of the geospatial cholera risk model for a 2-year period from January 2021 to December 2022. The cholera risk maps show considerable spatiotemporal variation across the landscape over these 2 years. The spatial variation in the cholera risk map for different months is due to monthly and seasonal variations in rainfall, temperature, and cholera prevalence, forecasted hydroclimatic variables as the same elevation and population density layers were used for every month. Generally, from December to May each year, low rainfall-induced water scarcity is associated with higher cholera risk in this region (Akanda et al., 2011; Nusrat & Akanda, 2019; Nusrat, Haque, et al., 2022; Nusrat, Khan, et al., 2022). The previous month's rainfall anomaly from December 2020 to February 2021 was generally high, positive values with some exceptions, indicating improved water supply situations compared to average conditions. Therefore, low cholera risks were

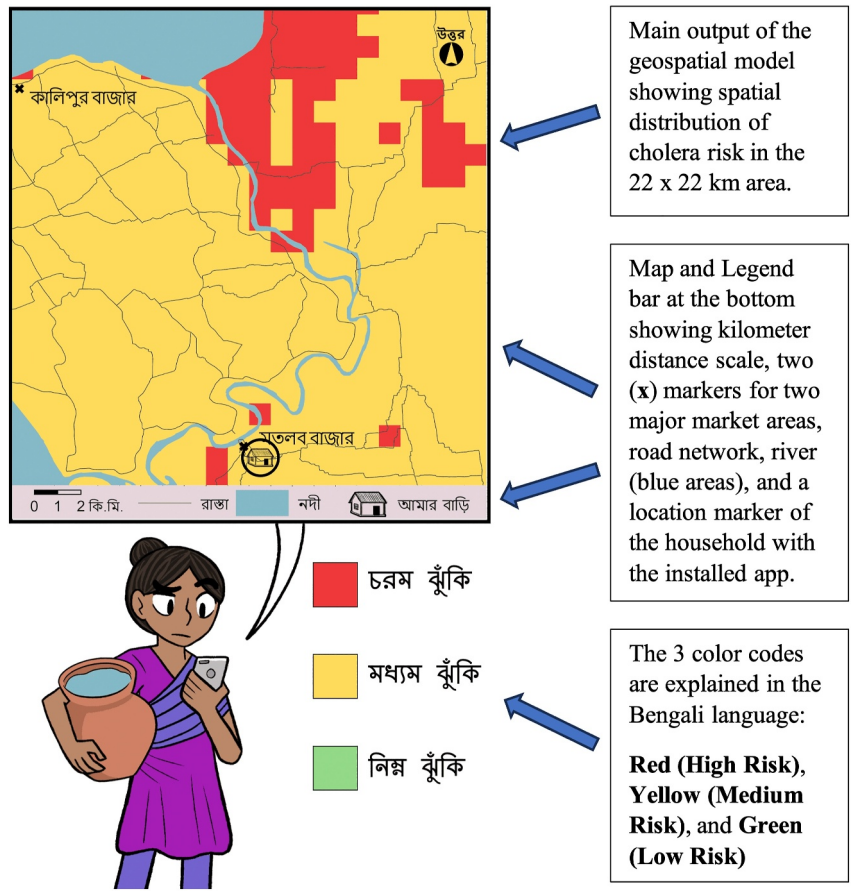

Figure 4. Example of monthly cholera risk map with detailed description.

observed during the spring 2021 season (March-April-May). The eastern side of the study area predominantly received less rainfall than the western side, which led to higher cholera risk predictions in the east.

For both years of 2021 and 2022, low values of forecasted rainfall were observed from November to March. As a result, high cholera risk values were observed during the subsequent dry months of April through June (Figure 5). If both past and present months have low rainfall, it implies increased odds of having high cholera risk as low rainfall increases pathogen intensity in waterbodies and also creates water scarcity, where people have to compromise their hygiene practices (Akanda et al., 2009; Koelle et al., 2005; Levy et al., 2016; Moors et al., 2013; Moran et al., 1997; Shehane et al., 2005). Low rainfall in the previous month or season increases pathogen concentration in waterbodies; the current month's high rainfall-induced runoff can then increase pathogen loads in waterbodies by washing out open defecation places, which is associated with cholera risk (Gaudart et al., 2013; Lloyd et al., 2007; Moors et al., 2013; Ruiz-Moreno et al., 2007; Singh et al., 2001). On the other hand, high forecasted rainfall values were seen between April and September leading to high cholera risk across the Matlab region for the post-monsoon period (October–November) in both years (Figures 5 and 6). Except for August 2021, considerable spatial variation of rainfall-induced cholera risk was observed during the study period. During the rainy period, higher rainfall is associated with higher cholera risk due to the potential for flooding and cross-contamination.

The temperature in the Matlab region shows a dual peak pattern similar to that of cholera risk. A positive temperature anomaly (higher temperature than the long-term mean) was observed during April and May. The temperature anomaly dropped between June to August and then increased starting in September. The temperature anomaly is high in spring and post-monsoon seasons and drops during the monsoon period due to high rainfall. The eastern side of the Matlab region experienced a positive temperature anomaly during April–May, which impacted the high cholera risk predictions found for May–June by causing higher evaporation, leading to less

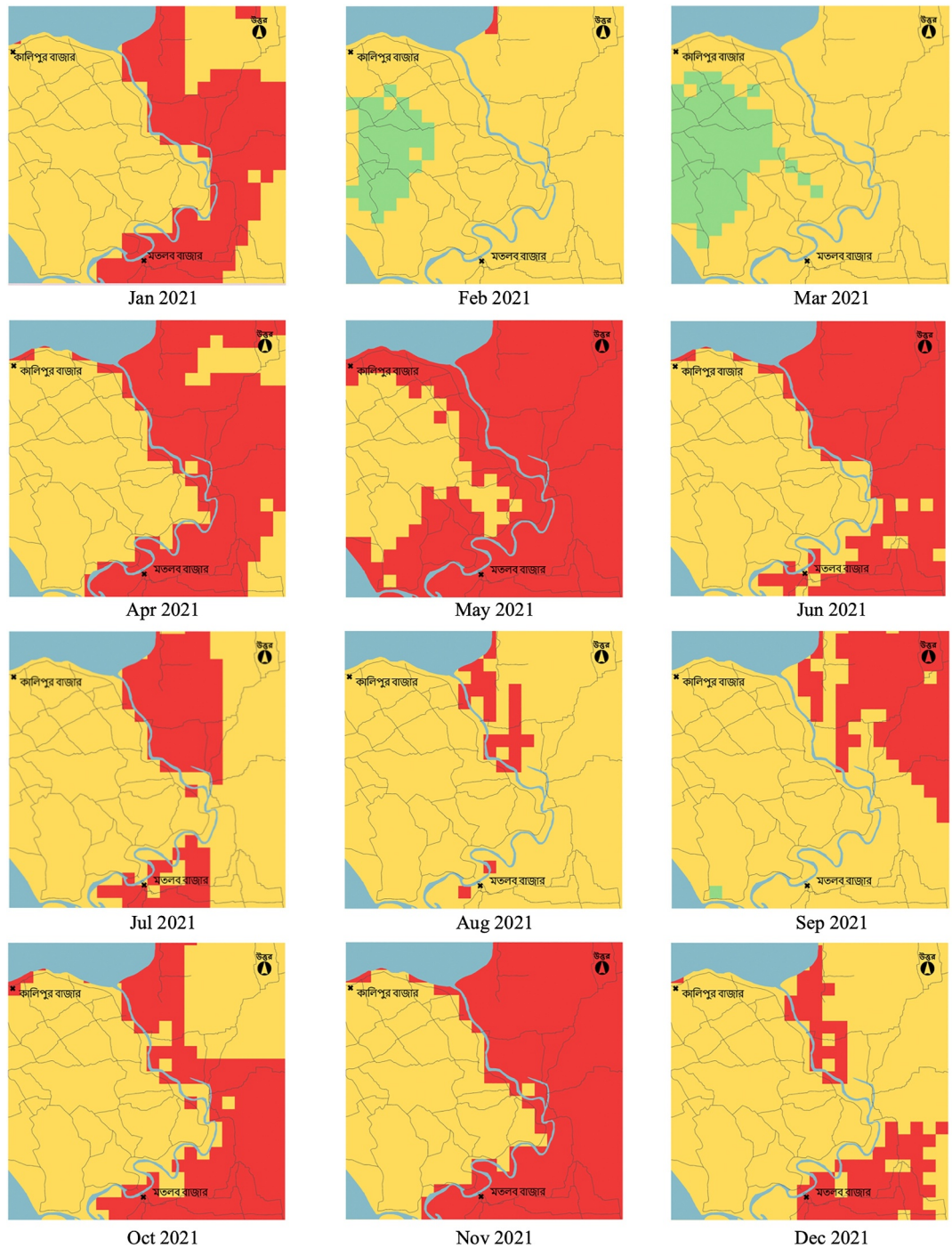

Figure 5. Monthly Cholera Risk for Matlab region, Bangladesh in 2021.

available water and also increasing the density of pathogens in few available waterbodies (Jutla et al., 2013). Despite experiencing a positive temperature anomaly, the western side showed only medium cholera risk, due to a lower population density. Similar to the rainfall forecasts, the spatial variation of the temperature forecasts is limited across the study area due to the spatial data resolution. However, an overall increase in temperature during the spring and post-monsoon months is observed and is associated with higher cholera risk.

The past month's cholera prevalence pattern is included in the risk analysis as cholera can have consecutive peaks in endemic settings (Codeço, 2001). The past month's average cholera prevalence also impacts the cholera risk

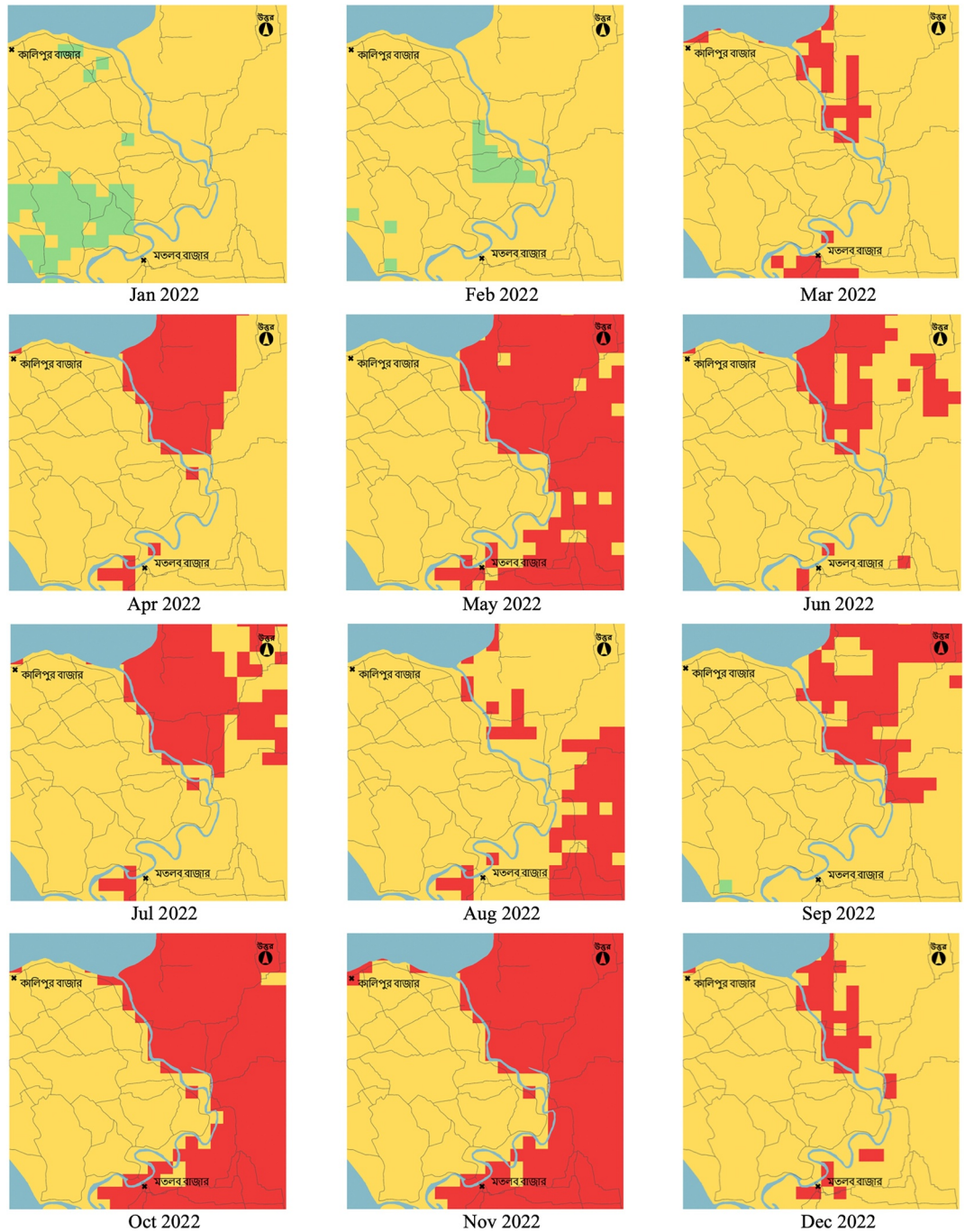

Figure 6. Monthly Cholera Risk for Matlab region, Bangladesh in 2022.

when it is considered along with other environmental variables. From March to May, cholera prevalence was high and that impacts the high cholera risk from April to June. Cholera prevalence drops from June to August during peak monsoon and fewer areas with high cholera risk are observed from July to September. This phenomenon has also been observed in previous studies on Bengal Delta cholera (Akanda et al., 2011; Huq et al., 2005; Sack et al., 2003). September and October months have high cholera prevalence, which is reflected in the cholera risk patterns seen for October and November months in both years (Figures 5 and 6).

3.2. Model Validation and Limitations

We evaluated the performance and the application of a geospatial cholera risk model as part of a cholera early warning system for Matlab, Bangladesh. There are several elements of cholera risk estimation in this study that require evaluation and validation of its analysis and accuracy. This model has been developed to simulate and forecast the varying risks and the temporal nature of cholera incidence in this historically endemic region. A major goal is to evaluate the spatial distribution and progression of risk in the study region, with the aim of identifying cholera *hotspots* or high-risk locations.

Another technical objective of this study is to investigate if high-resolution satellite-derived environmental data sets can be used to develop local-scale (*upazilla* or sub-district level) early warning models that can capture the spatiotemporal dynamics of waterborne disease risk in resource-constrained regions. Figures 5 and 6 show that the model successfully captures the spatial progression of cholera risk across the 22 km × 22 km region through the dry and wet seasons. The maps clearly show the seasonal progression of cholera risk through various parts of the region modulated by hydroclimatic drivers.

The presence of high-risk areas shown within these maps (such as cholera outbreak in Matlab Bazar in July and December 2021, and in the northeast quadrant in July 2021 and April 2022) shows the utility of such local-scale maps in identifying hotspot areas. To the best of our knowledge, this is the first combined instance of using earth observations data sets for cholera early warning at 1 km × 1 km resolution and delivered to users using a smartphone application. Due to the novel and recent nature of this study, there are no established data sets or health surveillance data sets that can be directly used for validation. However, our team was on the ground in Matlab Bazar during the ongoing cholera outbreak in December 2021. Although the month of December does not typically experience cholera in Matlab or elsewhere in Bangladesh, the field presence of our team in Matlab verified the occurrence of the increased cholera incidence in Matlab Upazilla hospital and corroborated the findings of our model, which successfully captures a cholera hotspot around the Matlab Bazar area in that unusual month. In addition, past publications on the regional incidence of cholera and other diarrheal diseases in the Matlab region strongly confirm a similar spatial pattern of outbreaks observed in the southwest (Matlab Bazar) and the northeast quadrant of the study region (Ali et al., 2002; Emch et al., 2008; Huq et al., 1984; Islam et al., 2009).

We also observed the effects of static information such as elevation and population density on cholera risk predictions for the four different quadrants of the study area. The eastern side mostly has a higher cholera risk than the western side due to higher population density. Overall, the highest cholera risks were observed in the northeast and the lowest risks were observed in the southwest (Figure S1 in Supporting Information S1). The northeast has high population density and low elevation, both of which contribute to high cholera risk predictions. The southwest, on the other hand, has lower population density and lower elevation (with some exceptions), leading to overall lower cholera risk predictions. However, the southwest had occasional outbreaks of strong magnitudes and these hotspots were captured by the model (Figures 5 and 6) and corroborated by past publications on flood vulnerability and cholera outbreaks in the region (Ali et al., 2002; Carrel et al., 2010; Emch et al., 2008).

An observed limitation of this model is that it seems to capture the high-risk areas more successfully than the low-risk areas. As a result, the model overestimates the risk in low cholera months. The Matlab region is long known to exhibit dual cholera peaks based on its historical surveillance records (Emch et al., 2008; Islam et al., 2009). Our results capture and illustrate both the spring and post-monsoon peaks and the increased intensity as well as the geographical spread of the outbreaks in the study region (Figure 7). As explained in Section 2.3, we adjusted model variables and their risk classification using a trial-and-error method to reflect on monthly patterns and capture the seasonal risk more accurately. The model captured high cholera risk from March to June, lower cholera risk during the monsoon, and increased risk again in September, peaking from October to November (Figure S2 in Supporting Information S1). These patterns successfully corroborated past publications on the spatiotemporal patterns of cholera in Matlab and its seasonal nature with respect to the hydroclimatic and environmental controls (Akanda et al., 2011, 2013; Carrel et al., 2010; Emch et al., 2010).

Figure 8 shows the monthly average of the calculated cholera risk index in comparison with historical Matlab cholera incidence data with a very similar shape in cholera progression through both seasons. The figure, however, shows the simulated peaks occurring about a month earlier, a signature of a shifting seasonality of cholera outbreaks. This phenomenon has been reported in recent publications as shifting hydrological as well as

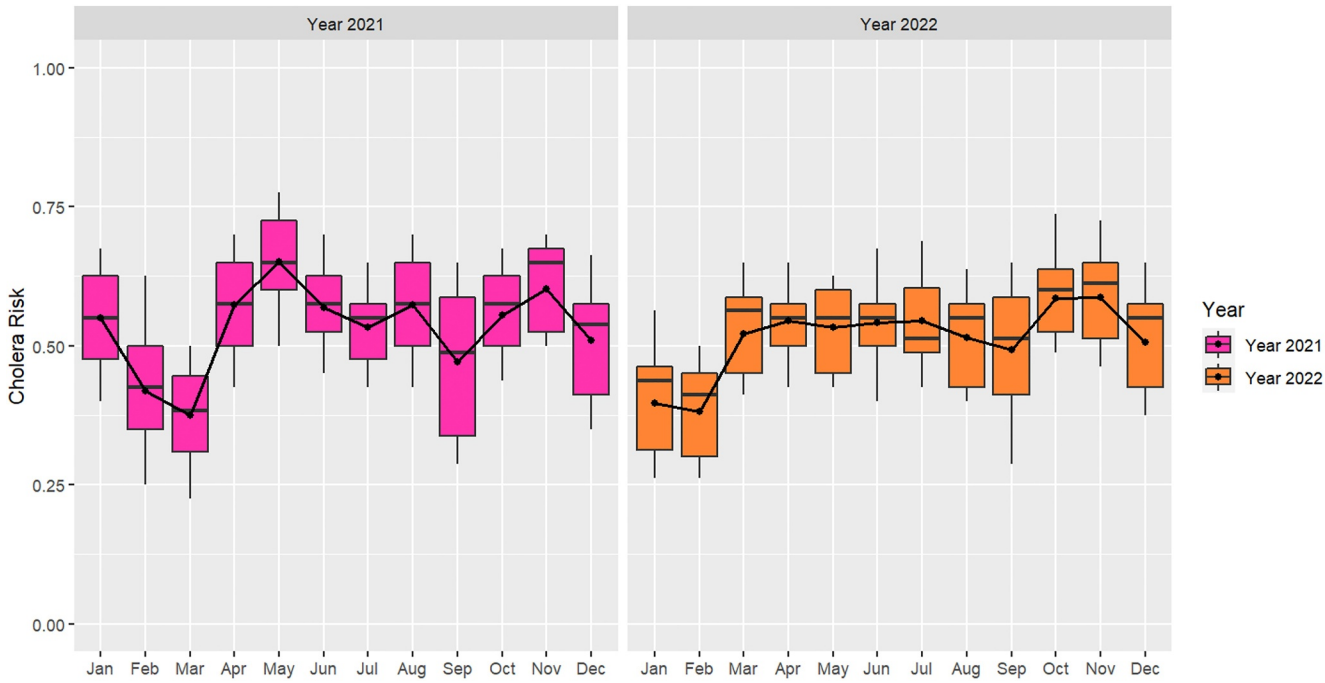

Figure 7. Monthly variation of cholera risk index in Matlab region for year 2021 and 2022.

epidemiological signatures of cholera in Bangladesh (Akanda et al., 2011; Chou et al., 2010; Daisy et al., 2020). A longer study period and accompanying cholera surveillance data sets would be required to confirm such changes in the environmental signals and potential effects on cholera signatures. This study thus supports the need for and contributes to producing spatially and temporally current information that varies during and by year versus comparison using long-term averages.

4. Conclusions

In this study, we developed a high-resolution geospatial model that used satellite remote sensing observations of environmental and hydroclimatic processes to calculate cholera transmission risk due to seasonal changes in the environment, natural hazards, and subsequent effects on water access and usage. In addition, we developed a mobile smartphone application to disseminate this information in the form of cholera risk maps to rural populations in a cholera-endemic region in South Asia—the Matlab region of Bangladesh.

The model captures the seasonal cholera pattern for the Matlab region satisfactorily. The outputs also provide a high-resolution understanding of the local-scale changes in cholera risk from month to month and within different parts of Matlab. Instead of fully relying on station-based hydroclimatological data, this study offers a new opportunity to use remote sensing data for designing and operating an early warning disease system. As cholera can spread very fast, creating an early warning system that can predict weekly cholera risk would provide even better management of the situation. Such high-resolution and spatial representation of cholera risk can readily help health workers in identifying at-risk regions and finding ways to allocate resources for recovery operations.

The cholera risk predictions were displayed in a geospatial and geocoded manner so that users could identify their own locations (pixel) on the map and understand the spatial nature of their surroundings' risks. The dynamic maps are updated each month to show the temporal change in cholera risk in each location as a function of seasonal environmental changes and regional weather influences. The smartphone application also provided further explanations about the risk of community transmission of cholera and different ways to prevent it and develop resilience against cholera by using safe water practices, adopting WASH protocols, and cleanliness in food preparation.

To the best of our knowledge, this study is the first attempt to combine the powers of satellites and smartphones for waterborne diarrheal diseases or water-related health applications. We have developed high-level, satellite-

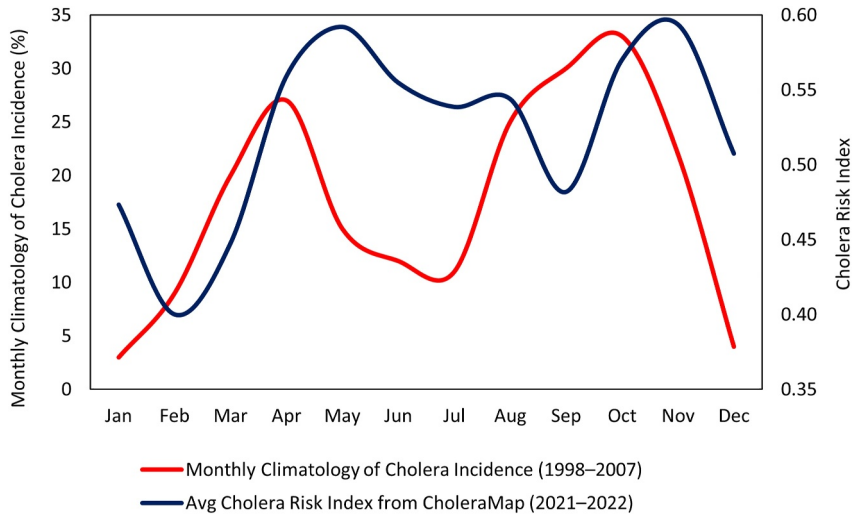

Figure 8. Comparison of recent monthly average cholera risk index (2021–2022) with past monthly average cholera incidence (%) (1998–2007) Data Source (Akanda et al., 2011).

derived, technical content and delivered it directly to non-technical, grassroots-level users, who otherwise have no access to technical water or personalized health risk information, using a smartphone application. This study is also the first attempt to change the traditional top-down technical information chain and directly empower vulnerable remote populations to make day-to-day decisions with an improved understanding of their water usage choices.

Early warning systems offer lead time to provide necessary interventions—for example, vaccination campaigns and providing water, sanitation and hygiene (WASH) facilities (Akanda et al., 2012, 2014). There are many ways to disseminate warnings including websites, mobile apps, television, radio, newspaper, and microphone announcements (remote areas with less access to technology)—thus, the dissemination process needs to be selected based on the targeted population and their accessibility to information. Despite disseminating the alert early, such a system may still fail due to a lack of coordination or proper decision-making protocols among public health officials (Council, 2001). Access to new technologies such as smartphones and accurate risk maps could potentially help provide clear instructions and strengthen policies toward effective information dissemination and management of responsibilities.

Conflict of Interest

The authors declare no conflicts of interest relevant to this study.

Data Availability Statement

Data: All earth observations and gridded data sets used in this study are collected from publicly available NASA (MODIS, IMERG, SEDAC) and other (USGS, NOAA) repositories (Table 1). Earth Observations of precipitation (IMERG) and temperature (MODIS) data used in this article are available in Huffman et al. (2019) and Wan et al. (2015, 2021), respectively. Rainfall and temperature forecasts are available from NOAA's North American Multi-Model Ensemble (NMME) project (Kirtman et al., 2014). Elevation data have been collected from the USGS HydroSHEDS project (Lehner et al., 2008). Population density data are available at SEDAC (CIESEN, 2018). Cholera data were obtained from the Ongoing Surveillance project at the Institute of Epidemiology, Disease Control and Research, Dhaka, Bangladesh (IEDCR, 2022). *Software*: The cholera risk model was developed using the ModelBuilder application of ArcGIS Desktop 10.7.1 (ESRI). The model and plotting codes are publicly available for download at Github (https://github.com/asakanda/CholeraMap.git). Canva, a graphic design platform, was used for creating Figure 3 (https://www.canva.com/).

Acknowledgments
The authors would like to thank the Grants for Assessing the Benefits of Satellites (GABS) program (Cooperative Agreement No. NNX17AD26A) as part of the Valuables Consortium– a joint initiative of the Resources for the Future Foundation (RFF) and the National Aeronautics and Space Administration (NASA) for providing core funds, and Moravian University for providing unrestricted support. F.N. and A.S.A were also supported by a grant from the NASA Health and Air Quality Program (Award No. 80NSSC22K1044) and from the University of Rhode Island Office of Research Development. We gratefully acknowledge the assistance of icddr,b, (particularly Ammatul Fardousi, Srizan Chowdhury, Mehedi Hasan, and Dr. Md. Al Fazal Khan) as well as the Governments of Bangladesh and Canada for providing core/unrestricted support to icddr,b.

References

Abdulrahim, A., & Adesola, R. O. (2022). Antimicrobial resistance in cholera: A need for quick intervention in Nigeria, West Africa. *International Journal of Travel Medicine and Global Health*, *10*(3), 99–103. https://doi.org/10.34172/ijtmgh.2022.18

Akanda, A. S., Jutla, A. S., Alam, M., De Magny, G. C., Siddique, A. K., Sack, R. B., et al. (2011). Hydroclimatic influences on seasonal and spatial cholera transmission cycles: Implications for public health intervention in the Bengal Delta. *Water Resources Research*, *47*(5), W00H07. https://doi.org/10.1029/2010WR009914

Akanda, A. S., Jutla, A. S., & Colwell, R. R. (2014). Global diarrhoea action plan needs integrated climate-based surveillance. *Lancet Global Health*, *2*(2), e69–e70. https://doi.org/10.1016/S2214-109X(13)70155-4

Akanda, A. S., Jutla, A. S., Gute, D. M., Evans, T., & Islam, S. (2012). Reinforcing cholera intervention through prediction-aided prevention. *Bulletin of the World Health Organization*, *90*(3), 243–244. https://doi.org/10.2471/blt.11.092189

Akanda, A. S., Jutla, A. S., Gute, D. M., Sack, R. B., Alam, M., Huq, A., et al. (2013). Population vulnerability to biannual cholera outbreaks and associated macro-scale drivers in the Bengal Delta. *The American Journal of Tropical Medicine and Hygiene*, *89*(5), 950–959. https://doi.org/10.4269/ajtmh.12-0492

Akanda, A. S., Jutla, A. S., & Islam, S. (2009). Dual peak cholera transmission in Bengal Delta: A hydroclimatological explanation. *Geophysical Research Letters*, *36*(19), L19401. https://doi.org/10.1029/2009GL039312

Alam, M., Islam, A., Bhuiyan, N., Rahim, N., Hossain, A., Khan, G. Y., et al. (2011). Clonal transmission, dual peak, and off-season cholera in Bangladesh. *Infection Ecology & Epidemiology*, *1*(1), 7273. https://doi.org/10.3402/iee.v1i0.7273

Alam, M., Sultana, M., Nair, G. B., Siddique, A. K., Hasan, N. A., Sack, R. B., et al. (2007). Viable but nonculturable *Vibrio cholerae* O1 in biofilms in the aquatic environment and their role in cholera transmission. *Proceedings of the National Academy of Sciences of the United States of America*, *104*(45), 17801–17806. https://doi.org/10.1073/pnas.0705599104

Alam, N., Ali, T., Razzaque, A., Rahman, M., Zahirul Haq, M., Saha, S. K., et al. (2017). Health and demographic surveillance system (HDSS) in Matlab, Bangladesh. *International Journal of Epidemiology*, *46*(3), 809–816. https://doi.org/10.1093/ije/dyx076

Ali, M., Emch, M., Donnay, J. P., Yunus, M., & Sack, R. B. (2002). Identifying environmental risk factors for endemic cholera: A raster GIS approach. *Health & Place*, *8*(3), 201–210. https://doi.org/10.1016/S1353-8292(01)00043-0

Ali, M., Kim, D. R., Yunus, M., & Emch, M. (2013). Time series analysis of cholera in Matlab, Bangladesh, during 1988-2001. *Journal of Health, Population and Nutrition*, *31*(1), 11. https://doi.org/10.3329/jhpn.v31i1.14744

Ali, M., Nelson, A. R., Lopez, A. L., & Sack, D. A. (2015). Updated global burden of cholera in endemic countries. *PLoS Neglected Tropical Diseases*, *9*(6), e0003832. https://doi.org/10.1371/journal.pntd.0003832

Anjumand, H. (2011). *Climate change: Bangladesh perspective*. Bangladesh Meteorological Department.

Asadgol, Z., Badirzadeh, A., Niazi, S., Mokhayeri, Y., Kermani, M., Mohammadi, H., & Gholami, M. (2020). How climate change can affect cholera incidence and prevalence? A systematic review. *Environmental Science and Pollution Research*, *27*(28), 34906–34926. https://doi.org/10.1007/s11356-020-09992-7

Asadgol, Z., Mohammadi, H., Kermani, M., Badirzadeh, A., & Gholami, M. (2019). The effect of climate change on cholera disease: The road ahead using artificial neural network. *PLoS One*, *14*(11), e0224813. https://doi.org/10.1371/journal.pone.0224813

Baker-Austin, C., Oliver, J. D., Alam, M., Ali, A., Waldor, M. K., Qadri, F., & Martinez-Urtaza, J. (2018). Vibrio spp. infections. *Nature Reviews Disease Primers*, *4*(1), 1–19. https://doi.org/10.1038/s41572-018-0005-8

Batabyal, P., Mookerjee, S., Einsporn, M. H., Lara, R. J., & Palit, A. (2014). High prevalence of toxin producing enteropathogenic Vibrios among estuarine crab in Ganges delta of West Bengal, India. *Infection, Genetics and Evolution*, *26*, 359–361. https://doi.org/10.1016/j.meegid.2014.06.001

Brooks, W. A., Zaman, K., Goswami, D., Prosperi, C., Endtz, H. P., Hossain, L., et al. (2021). The etiology of childhood pneumonia in Bangladesh: Findings from the Pneumonia Etiology Research for Child Health (PERCH) study. *The Pediatric Infectious Disease Journal*, *40*(9), S79–S90. https://doi.org/10.1097/inf.0000000000002648

Call, M. A., Gray, C., Yunus, M., & Emch, M. (2017). Disruption, not displacement: Environmental variability and temporary migration in Bangladesh. *Global Environmental Change*, *46*, 157–165. https://doi.org/10.1016/j.gloenvcha.2017.08.008

Camacho, A., Bouhenia, M., Alyusfi, R., Alkohlani, A., Naji, M. A. M., de Radiguès, X., et al. (2018). Cholera epidemic in Yemen, 2016–18: An analysis of surveillance data. *Lancet Global Health*, *6*(6), e680–e690. https://doi.org/10.1016/s2214-109x(18)30230-4

Campbell, A. M., Racault, M.-F., Goult, S., & Laurenson, A. (2020). Cholera risk: A machine learning approach applied to essential climate variables. *International Journal of Environmental Research and Public Health*, *17*(24), 9378. https://doi.org/10.3390/ijerph17249378

Carrel, M., Voss, P., Streatfield, P. K., Yunus, M., & Emch, M. (2010). Protection from annual flooding is correlated with increased cholera prevalence in Bangladesh: A zero-inflated regression analysis. *Environmental Health*, *9*(1), 1–9. https://doi.org/10.1186/1476-069x-9-13

Chamanrokh, P., Colwell, R. R., & Huq, A. (2022). Loop-mediated isothermal amplification (LAMP) assay for rapid detection of viable but non-culturable *Vibrio cholerae* O1. *Canadian Journal of Microbiology*, *68*(2), 103–110. https://doi.org/10.1139/cjm-2021-0142

Chou, W. C., Wu, J. L., Wang, Y. C., Huang, H., Sung, F. C., & Chuang, C. Y. (2010). Modeling the impact of climate variability on diarrhea-associated diseases in Taiwan (1996-2007). *Science of the Total Environment*, *409*(1), 43–51. https://doi.org/10.1016/j.scitotenv.2010.09.001

Christaki, E., Dimitriou, P., Pantavou, K., & Nikolopoulos, G. K. (2020). The impact of climate change on Cholera: A review on the global status and future challenges. *Atmosphere*, *11*(5), 449. https://doi.org/10.3390/atmos11050449

CIESIN (Center for International Earth Science Information Network) - Columbia University. (2018). *Gridded population of the world, version 4 (GPWv4): Population density, revision 11*. NASA Socioeconomic Data and Applications Center (SEDAC). https://doi.org/10.7927/H49C6VHW

Codeço, C. T. (2001). Endemic and epidemic dynamics of cholera: The role of the aquatic reservoir. *BMC Infectious Diseases*, *1*(1), 1–14. https://doi.org/10.1186/1471-2334-1-1

Colwell, R. R., Brayton, P., Herrington, D., Tall, B., Huq, A., & Levine, M. M. (1996). Viable but non-culturable *Vibrio cholerae* O1 revert to a cultivable state in the human intestine. *World Journal of Microbiology and Biotechnology*, *12*(1), 28–31. https://doi.org/10.1007/bf00327795

Constantin de Magny, G., Murtugudde, R., Sapiano, M. R. P., Nizam, A., Brown, C. W., Busalacchi, A. J., et al. (2008). Environmental signatures associated with cholera epidemics. *Proceedings of the National Academy of Sciences of the United States of America*, *105*(46), 17676–17681. https://doi.org/10.1073/pnas.0809654105

Costello, A., Abbas, M., Allen, A., Ball, S., Bell, S., Bellamy, R., et al. (2009). Managing the health effects of climate change: Lancet and University College London Institute for Global Health Commission. *The Lancet*, *373*(9676), 1693–1733. https://doi.org/10.1016/s0140-6736(09)60935-1

Council, N. R. (2001). *Under the weather: Climate, ecosystems, and infectious disease*. National Academies Press. Retrieved from https://www.ncbi.nlm.nih.gov/books/NBK222241/

Craig, R. K. (2018). Cholera and climate change: Pursuing public health adaptation strategies in the face of scientific debate. *Houston Journal of Health Law & Policy*, *18*, 29.

Daisy, S. S., Saiful Islam, A. K. M., Akanda, A. S., Faruque, A. S. G., Amin, N., & Jensen, P. K. M. (2020). Developing a forecasting model for cholera incidence in Dhaka megacity through time series climate data. *Journal of Water and Health*, *18*(2), 207–223. https://doi.org/10.2166/wh.2020.133

Doblas-Reyes, F. J., Hagedorn, R., & Palmer, T. N. (2005). The rationale behind the success of multi-model ensembles in seasonal forecasting—II. Calibration and combination. *Tellus A: Dynamic Meteorology and Oceanography*, *57*(3), 234–252. https://doi.org/10.1111/j.1600-0870.2005.00104.x

Dvorak, A. C., Solo-Gabriele, H. M., Galletti, A., Benzecry, B., Malone, H., Boguszewski, V., & Bird, J. (2018). Possible impacts of sea level rise on disease transmission and potential adaptation strategies, a review. *Journal of Environmental Management*, *217*, 951–968. https://doi.org/10.1016/j.jenvman.2018.03.102

Elnemr, W. M. (2014). *Environmental cholera transmission triggers in Delta Bengal*. University of Maryland.

Emch, M., Feldacker, C., Yunus, M., Streatfield, P. K., DinhThiem, V., Canh, D. G., et al. (2008). Local environmental predictors of cholera in Bangladesh and Vietnam. *The American Journal of Tropical Medicine and Hygiene*, *78*(5), 823–832. https://doi.org/10.4269/ajtmh.2008.78.823

Emch, M., Yunus, M., Escamilla, V., Feldacker, C., & Ali, M. (2010). Local population and regional environmental drivers of cholera in Bangladesh. *Environmental Health*, *9*(1), 1–8. https://doi.org/10.1186/1476-069x-9-2

Farmer, P., Almazor, C. P., Bahnsen, E. T., Barry, D., Bazile, J., Bloom, B. R., et al. (2011). Meeting cholera's challenge to Haiti and the world: A joint statement on cholera prevention and care. *PLoS Neglected Tropical Diseases*, *5*(5), e1145. https://doi.org/10.1371/journal.pntd.0001145

Finger, F., Genolet, T., Mari, L., de Magny, G. C., Manga, N. M., Rinaldo, A., & Bertuzzo, E. (2016). Mobile phone data highlights the role of mass gatherings in the spreading of cholera outbreaks. *Proceedings of the National Academy of Sciences of the United States of America*, *113*(23), 6421–6426. https://doi.org/10.1073/pnas.1522305113

Gabutti, G., Rossanese, A., Tomasi, A., Giuffrida, S., Nicosia, V., Barriga, J., et al. (2020). Cholera, the current status of cholera vaccines and recommendations for travellers. *Vaccines*, *8*(4), 606. https://doi.org/10.3390/vaccines8040606

Gaudart, J., Rebaudet, S., Barrais, R., Boncy, J., Faucher, B., Piarroux, M., et al. (2013). Spatio-temporal dynamics of cholera during the first year of the epidemic in Haiti. *PLoS Neglected Tropical Diseases*, *7*(4), e2145. https://doi.org/10.1371/journal.pntd.0002145

Griffith, D. C., Kelly-Hope, L. A., & Miller, M. A. (2006). Review of reported cholera outbreaks worldwide, 1995–2005. *The American Journal of Tropical Medicine and Hygiene*, *75*(5), 973–977. https://doi.org/10.4269/ajtmh.2006.75.973

Hagedorn, R., Doblas-Reyes, F. J., & Palmer, T. N. (2005). The rationale behind the success of multi-model ensembles in seasonal forecasting—I. Basic concept. *Tellus A: Dynamic Meteorology and Oceanography*, *57*(3), 219–233. https://doi.org/10.3402/tellusa.v57i3.14657

Haq, M. Z., Alam, S., Haider, M., Rahman, M., Mustafa, A. H. M., Saha, S. K., et al. (2018). Health and demographic surveillance system–Matlab, v. 51. Registration of health and demographic events 2016.

Hashizume, M., Faruque, A. S. G., Wagatsuma, Y., Hayashi, T., & Armstrong, B. (2010). Cholera in Bangladesh: Climatic components of seasonal variation. *Epidemiology*, *21*(5), 706–710. https://doi.org/10.1097/ede.0b013e3181e5b053

Hiremath, N. S., Cattamanchi, S., Vidyalakshmi, P. R., & Trounce, M. (2015). Vibrio cholerae *(cholera) attack* (pp. 724–725). Ciottone's Disaster Medicine; Elsevier Inc.

Huffman, G. J., Stocker, E. F., Bolvin, D. T., Nelkin, E. J., & Tan, J. (2019). *GPM IMERG late precipitation L3 1 day 0.1 degree x 0.1 degree V06*. In A. Savtchenko (Ed.), Goddard Earth Sciences Data and Information Services Center. https://doi.org/10.5067/GPM/IMERGDL/DAY/06

Huq, A., Sack, R. B., Nizam, A., Longini, I. M., Nair, G. B., Ali, A., et al. (2005). Critical factors influencing the occurrence of *Vibrio cholerae* in the environment of Bangladesh. *Applied and Environmental Microbiology*, *71*(8), 4645–4654. https://doi.org/10.1128/aem.71.8.4645-4654.2005

Huq, A., West, P. A., Small, E. B., Huq, M. I., & Colwell, R. R. (1984). Influence of water temperature, salinity, and pH on survival and growth of toxigenic *Vibrio cholerae* serovar O1 associated with live copepods in laboratory microcosms. *Applied and Environmental Microbiology*, *48*(2), 420–424. https://doi.org/10.1128/aem.48.2.420-424.1984

Hussain-Alkhateeb, L., Rivera Ramirez, T., Kroeger, A., Gozzer, E., & Runge-Ranzinger, S. (2021). Early warning systems (EWSs) for chikungunya, dengue, malaria, yellow fever, and Zika outbreaks: What is the evidence? A scoping review. *PLoS Neglected Tropical Diseases*, *15*(9), e0009686. https://doi.org/10.1371/journal.pntd.0009686

IEDCR (Institute of Epidemiology, Disease Control and Research). (2022). Ongoing surveillance at IEDCR—Cholera surveillance. Retrieved from https://old.iedcr.gov.bd/index.php/surveillance

Islam, M. S., Sharker, M. A. Y., Rheman, S., Hossain, S., Mahmud, Z. H., Islam, M. S., et al. (2009). Effects of local climate variability on transmission dynamics of cholera in Matlab, Bangladesh. *Transactions of the Royal Society of Tropical Medicine and Hygiene*, *103*(11), 1165–1170. https://doi.org/10.1016/j.trstmh.2009.04.016

Jutla, A., Aldaach, H., Billian, H., Akanda, A., Huq, A., & Colwell, R. (2015). Satellite based assessment of hydroclimatic conditions related to cholera in Zimbabwe. *PLoS One*, *10*(9), e0137828. https://doi.org/10.1371/journal.pone.0137828

Jutla, A., Usmani, M., Brumfield, K. D., Singh, K., McBean, F., Potter, A., et al. (2023). Anticipatory decision-making for cholera in Malawi. *Mbio*, *14*(6), e00529-23. https://doi.org/10.1128/mbio.00529-23

Jutla, A., Whitcombe, E., Hasan, N., Haley, B., Akanda, A., Huq, A., et al. (2013). Environmental factors influencing epidemic cholera. *The American Journal of Tropical Medicine and Hygiene*, *89*(3), 597–607. https://doi.org/10.4269/ajtmh.12-0721

Khan, R., Aldaach, H., McDonald, C., Alam, M., Huq, A., Gao, Y., et al. (2019). Estimating cholera risk from an exploratory analysis of its association with satellite-derived land surface temperatures. *International Journal of Remote Sensing*, *40*(13), 4898–4909. https://doi.org/10.1080/01431161.2019.1577575

Khan, R., Anwar, R., Akanda, S., McDonald, M. D., Huq, A., Jutla, A., & Colwell, R. (2017). Assessment of risk of cholera in Haiti following Hurricane Matthew. *The American Journal of Tropical Medicine and Hygiene*, *97*(3), 896–903. https://doi.org/10.4269/ajtmh.17-0048

Kirtman, B. P., & Min, D. (2009). Multimodel ensemble ENSO prediction with CCSM and CFS. *Monthly Weather Review*, *137*(9), 2908–2930. https://doi.org/10.1175/2009mwr2672.1

Kirtman, B. P., Min, D., Infanti, J. M., KinterIII, J. L., Paolino, D. A., Zhang, Q., et al. (2014). The North American Multi-Model Ensemble (NMME): Phase-1 seasonal to interannual prediction; Phase-2 toward developing intra-seasonal prediction. *Bulletin of the American Meteorological Society*, *95*(4), 585–601. https://doi.org/10.1175/BAMS-D-12-00050.1

Koelle, K., Rodó, X., Pascual, M., Yunus, M., & Mostafa, G. (2005). Refractory periods and climate forcing in cholera dynamics. *Nature*, *436*(7051), 696–700. https://doi.org/10.1038/nature03820

Lehner, B., Verdin, K., & Jarvis, A. (2008). New global hydrography derived from spaceborne elevation data. *Eos, Transactions American Geophysical Union*, *89*(10), 93–94. https://doi.org/10.1029/2008EO100001

Levy, K., Woster, A. P., Goldstein, R. S., & Carlton, E. J. (2016). Untangling the impacts of climate change on waterborne diseases: A systematic review of relationships between diarrheal diseases and temperature, rainfall, flooding, and drought. *Environmental Science and Technology*, *50*(10), 4905–4922. https://doi.org/10.1021/acs.est.5b06186

Lloyd, S. J., Kovats, R. S., & Armstrong, B. G. (2007). Global diarrhoea morbidity, weather and climate. *Climate Research*, *34*(2), 119–127. https://doi.org/10.3354/cr034119

Lobitz, B., Beck, L., Huq, A., Wood, B., Fuchs, G., Faruque, A. S. G., & Colwell, R. (2000). Climate and infectious disease: Use of remote sensing for detection of *Vibrio cholerae* by indirect measurement. *Proceedings of the National Academy of Sciences of the United States of America*, *97*(4), 1438–1443. https://doi.org/10.1073/pnas.97.4.1438

Longini, I. M., Jr., Yunus, M., Zaman, K., Siddique, A. K., Sack, R. B., & Nizam, A. (2002). Epidemic and endemic cholera trends over a 33-year period in Bangladesh. *The Journal of Infectious Diseases*, *186*(2), 246–251. https://doi.org/10.1086/341206

Louis, V. R., Russek-Cohen, E., Choopun, N., Rivera, I. N. G., Gangle, B., Jiang, S. C., et al. (2003). Predictability of *Vibrio cholerae* in Chesapeake Bay. *Applied and Environmental Microbiology*, *69*(5), 2773–2785. https://doi.org/10.1128/AEM.69.5.2773-2785.2003

Luque Fernandez, M. A., Schomaker, M., Mason, P. R., Fesselet, J. F., Baudot, Y., Boulle, A., & Maes, P. (2012). Elevation and cholera: An epidemiological spatial analysis of the cholera epidemic in Harare, Zimbabwe, 2008-2009. *BMC Public Health*, *12*(1), 1–8. https://doi.org/10.1186/1471-2458-12-442

Manandhar, A., Fischer, A., Bradley, D. J., Salehin, M., Islam, M. S., Hope, R., & Clifton, D. A. (2020). Machine learning to evaluate impacts of flood protection in Bangladesh, 1983–2014. *Water*, *12*(483), 483. https://doi.org/10.3390/w12020483

Mason, P. R. (2009). Zimbabwe experiences the worst epidemic of cholera in Africa. *The Journal of Infection in Developing Countries*, *3*(02), 148–151. https://doi.org/10.3855/jidc.62

Moore, S. M., Azman, A. S., Zaitchik, B. F., Mintz, E. D., Brunkard, J., Legros, D., et al. (2017). El Niño and the shifting geography of cholera in Africa. *Proceedings of the National Academy of Sciences of the United States of America*, *114*(17), 4436–4441. https://doi.org/10.1073/pnas.1617218114

Moors, E., Singh, T., Siderius, C., Balakrishnan, S., & Mishra, A. (2013). Climate change and waterborne diarrhoea in northern India: Impacts and adaptation strategies. *Science of the Total Environment*, *468–469*, S139–S151. https://doi.org/10.1016/j.scitotenv.2013.07.021

Moran, P., Nhandara, C., Hove, I., Charimari, L., Katito, C., Bradley, M., & Williams, M. A. (1997). Contamination of traditional drinking water sources during a period of extreme drought in the Zvimba communal lands, Zimbabwe. *Central African Journal of Medicine*, *43*(11), 316–321.

Nusrat, F., & Akanda, A. S. (2019). Understanding the impact of hydrological processes and climatic extremes on acute diarrheal disease prevalence in regions suffering from water insecurity. In *AGU fall meeting abstracts, 2019*, GH33B-1200.

Nusrat, F., Haque, M., Rollend, D., Christie, G., & Akanda, A. S. (2022). A high-resolution earth observations and machine learning-based approach to forecast waterborne disease risk in post-disaster settings. *Climate*, *10*(4), 48. https://doi.org/10.3390/cli10040048

Nusrat, F., Khan, A. I., Islam, M. T., Qadri, F., & Akanda, A. S. (2022). Utilizing Earth observations to understand the impacts of water security and hydroclimatological extremes on acute watery diarrhea (AWD). In *AGU fall meeting abstracts*. GH15D-0470.

Pakhtigian, E. L., Aziz, S., Boyle, K., Akanda, A. S., & Hanifi, M. A. (2022). Early warning systems, mobile technology, and cholera aversion: Evidence from rural Bangladesh. *Journal of Environmental Economics and Management*, *125*(2024), 102966. https://doi.org/10.1016/j.jeem.2024.102966

Palash, W., Jiang, Y., Akanda, A. S., Small, D. L., Nozari, A., & Islam, S. (2018). A streamflow and water level forecasting model for the Ganges, Brahmaputra, and Meghna rivers with requisite simplicity. *Journal of Hydrometeorology*, *19*(1), 201–225. https://doi.org/10.1175/jhm-d-16-0202.1

Pascual, M., Rodó, X., Ellner, S. P., Colwell, R., & Bouma, M. J. (2000). Cholera dynamics and El Nino-southern oscillation. *Science*, *289*(5485), 1766–1769. https://doi.org/10.1126/science.289.5485.1766

Reyburn, R., Kim, D. R., Emch, M., Khatib, A., Von Seidlein, L., & Ali, M. (2011). Climate variability and the outbreaks of cholera in Zanzibar, East Africa: A time series analysis. *The American Journal of Tropical Medicine and Hygiene*, *84*(6), 862–869. https://doi.org/10.4269/ajtmh.2011.10-0277

Rinaldo, A., Bertuzzo, E., Mari, L., Righetto, L., Blokesch, M., Gatto, M., et al. (2012). Reassessment of the 2010–2011 Haiti cholera outbreak and rainfall-driven multiseason projections. *Proceedings of the National Academy of Sciences of the United States of America*, *109*(17), 6602–6607. https://doi.org/10.1073/pnas.1203333109

Root, G. (1997). Population density and spatial differentials in child mortality in Zimbabwe. *Social Science & Medicine*, *44*(3), 413–421. https://doi.org/10.1016/S0277-9536(96)00162-1

Ruiz-Moreno, D., Pascual, M., Bouma, M., Dobson, A., & Cash, B. (2007). Cholera seasonality in Madras (1901–1940): Dual role for rainfall in endemic and epidemic regions. *EcoHealth*, *4*(1), 52–62. https://doi.org/10.1007/s10393-006-0079-8

Sack, D. A., Debes, A. K., Ateudjieu, J., Bwire, G., Ali, M., Ngwa, M. C., et al. (2021). Contrasting epidemiology of Cholera in Bangladesh and Africa. *Journal of Infectious Diseases*, *224*(Supplement_7), S701–S709. https://doi.org/10.1093/infdis/jiab440

Sack, D. A., Sack, R. B., Nair, G. B., & Siddique, A. (2004). Cholera. *Cholera Lancet*, *363*(9404), 233. https://doi.org/10.1016/s0140-6736(03)15328-7

Sack, R. B., Siddique, A. K., Longini, I. M., Jr., Nizam, A., Yunus, M., Islam, M. S., et al. (2003). A 4-year study of the epidemiology of *Vibrio cholerae* in four rural areas of Bangladesh. *The Journal of Infectious Diseases*, *187*(1), 96–101. https://doi.org/10.1086/345865

Saha, S., Halder, M., Mookerjee, S., & Palit, A. (2019). Seasonal influence, enteropathogenic microbial load and diarrhoeal enigma in the Gangetic Delta, India: Present scenario and health implications. *Journal of Infection and Public Health*, *12*(4), 540–548. https://doi.org/10.1016/j.jiph.2019.01.066

Shehane, S. D., Harwood, V. J., Whitlock, J. E., & Rose, J. B. (2005). The influence of rainfall on the incidence of microbial faecal indicators and the dominant sources of faecal pollution in a Florida river. *Journal of Applied Microbiology*, *98*(5), 1127–1136. https://doi.org/10.1111/j.1365-2672.2005.02554.x

Siddique, A. K., Zaman, K., Baqui, A. H., Akram, K., Mutsuddy, P., Eusof, A., et al. (1992). Cholera epidemics in Bangladesh: 1985-1991. *Journal of Diarrhoeal Diseases Research*, *10*(2), 79–86.

Silva, A. J., & Benitez, J. A. (2016). *Vibrio cholerae* biofilms and cholera pathogenesis. *PLoS Neglected Tropical Diseases*, *10*(2), e0004330. https://doi.org/10.1371/journal.pntd.0004330

Singh, R. B. K., Hales, S., De Wet, N., Raj, R., Hearnden, M., & Weinstein, P. (2001). The influence of climate variation and change on diarrheal disease in the Pacific Islands. *Environmental Health Perspectives*, *109*(2), 155–159. https://doi.org/10.1289/ehp.01109155

Sit, B., Fakoya, B., & Waldor, M. K. (2022). Emerging concepts in cholera vaccine design. *Annual Review of Microbiology*, *76*(1), 681–702. https://doi.org/10.1146/annurev-micro-041320-033201

Slater, L. J., Villarini, G., & Bradley, A. A. (2017). Weighting of NMME temperature and precipitation forecasts across Europe. *Journal of Hydrology*, *552*, 646–659. https://doi.org/10.1016/j.jhydrol.2017.07.029

Smirnova, A., Sterrett, N., Mujica, O. J., Munayco, C., Suárez, L., Viboud, C., & Chowell, G. (2020). Spatial dynamics and the basic reproduction number of the 1991–1997 cholera epidemic in Peru. *PLoS Neglected Tropical Diseases*, *14*(7), e0008045. https://doi.org/10.1371/journal.pntd.0008045

Tamplin, M. L., Gauzens, A. L., Huq, A., Sack, D. A., & Colwell, R. (1990). Attachment of *Vibrio cholerae* serogroup O1 to zooplankton and phytoplankton of Bangladesh waters. *Applied and Environmental Microbiology*, *56*(6), 1977–1980. https://doi.org/10.1128/aem.56.6.1977-1980.1990

Taneja, N., Mishra, A., Batra, N., Gupta, P., Mahindroo, J., & Mohan, B. (2020). Inland cholera in freshwater environs of North India. *Vaccine*, *38*, A63–A72. https://doi.org/10.1016/j.vaccine.2019.06.038

Usmani, M., Brumfield, K. D., Magers, B. M., Chaves-Gonzalez, J., Ticehurst, H., Barciela, R., et al. (2023). Combating cholera by building predictive capabilities for pathogenic *Vibrio cholerae* in Yemen. *Scientific Reports*, *13*(1), 2255. https://doi.org/10.1038/s41598-022-22946-y

Wan, Z., Hook, S., & Hulley, G. (2015). MOD11C3 MODIS/Terra land surface temperature/emissivity monthly L3 global 0.05Deg CMG V006 [Dataset]. *NASA EOSDIS Land Processes Distributed Active Archive Center*. https://doi.org/10.5067/MODIS/MOD11C3.006

Wan, Z., Hook, S., & Hulley, G. (2021). MODIS/Terra land surface temperature/emissivity daily L3 global 1km SIN Grid V061 [Dataset]. *NASA EOSDIS Land Processes Distributed Active Archive Center*. https://doi.org/10.5067/MODIS/MOD11A1.061

WHO. (2022). Cholera. Retrieved from https://www.who.int/news-room/fact-sheets/detail/cholera

Xu, M., Cao, C. X., Wang, D. C., Kan, B., Xu, Y. F., Ni, X. L., & Zhu, Z. C. (2016). Environmental factor analysis of cholera in China using remote sensing and geographical information systems. *Epidemiology and Infection*, *144*(5), 940–951. https://doi.org/10.1017/s095026881500223x

Zarocostas, J. (2009). *Aid organisations warn Zimbabwe's cholera crisis is far from over*. British Medical Journal Publishing Group.